ISBN: 978-3-95450-188-5 doi:10.18429/JACoW-MEDSI2016-TUPE10

A THERMAL EXPLORATION OF DIFFERENT MONOCHROMATOR CRYSTAL DESIGNS

J. S. Stimson†, M. Ward, Birmingham City University, Birmingham, United Kingdom
S. Diaz-Moreno, P. Docker, J. Kay, J. Sutter, Diamond Light Source, Didcot, United Kingdom

Abstract

Eight potential monochromator crystal designs were subjected to a combination of three different beam powers on two different footprints. The temperature and thermal deformation were determined for each. It was found that thermal deformation of the lattice is negligible compared to the surface curvature, and that while the thinnest crystal wafer showed the smallest temperature increase, crystals cooled from the bottom alone demonstrated a far more uniform thermal deformation and a larger radius of curvature.

INTRODUCTION

In this work we have explored various monochromator crystal designs. Monochromator crystals are used to select a single wavelength of x-rays from the broad spectrum produced in a synchrotron device [1-2]. The high energies these crystals are subjected to causes them to heat up significantly, leading to thermal deformations that distort the uniform surface of the crystal, leading to multiple wavelengths being selected [3-4]. This is problematic as it is not always obvious whether the change in wavelength at the detector is due to thermal distortion of the monochromator or interaction with the sample being tested.

In order to attempt to reduce or even eliminate this thermal deformation it must be understood how different variables affect the system. To this end we have modelled several different designs of monochromator crystal to see what effect changing the geometry has on the thermal deformation.

As we are concerned primarily with thermal behaviours, we have made a number of approximations. The cooled surfaces remain at 80 K throughout to approximate the flow of liquid nitrogen with an ideal thermal contact [5]. This is a very non-physical boundary condition, which means the results are not directly comparable to real world systems. However, for the purpose of this work it has been used to create a directly comparable baseline between the different models.

It is also assumed that each crystal has thermalized prior to exposure to the beam, and therefore is initially at a uniform temperature of 80 K.

Three beam powers were considered; 110 Watts, 550 Watts and 1100 Watts. This was to simulate exposure to low power, high power and future high power beams as used at the Diamond Light Source. Each of these powers had to be applied using the Beer-Lambert law of beam transmission [6], as shown in Eq. (1) below.

$$I = I_0\, e^{-\mu x} \tag{1}$$

In Eq. (1) I is the intensity of the beam, I_0 is the intensity of the beam at the surface, μ is the absorption coefficient and x is the distance into the material.

As the beam produced by the I20 beamline is broad spectrum, this calculation was done for each energy and then integrated across all energies as shown in Eq. (2).

$$I = \int I_0(E) e^{-\mu(E)x}\, dE \tag{2}$$

In Eq. (2) I_0 (E) is the intensity of the beam at the surface for x-rays of a given energy and μ(E) is the absorption coefficient for x-rays of the given energy in silicon.

This was done for the measured intensities of each wavelength at the I20 beamline for the given power values. The intensity penetrates the surface, decreasing as it propagates.

Two major factors were considered; the deformation of the diffracting surface could change both the spacing of the lattice layers and change the angle of incidence, both of which can damage the Bragg diffraction desired by modifying lattice layer structure [1].

These are only an issue if they are non-uniform across the diffracting surface, as a uniform change can be allowed for when angling the monochromator crystal. As such the radius of curvature of the diffracting surface has been calculated at the centre of the surface for each design.

The curvature, k, can be calculated by mapping some function y to the deformation of the surface, then applying Eq. 3 [7].

$$k = \frac{\left(\frac{d^2y}{dx^2}\right)^{\frac{3}{2}}}{1+\left(\frac{dy}{dx}\right)^2} \tag{3}$$

The radius of curvature is simply the reciprocal of the modulus of curvature [7], as shown in Eq. 4.

$$R = \frac{1}{|k|} \tag{4}$$

A larger radius of curvature relates to a flatter crystal surface, i.e. the larger the radius of curvature the better.

The lattice spacing as a function of temperature was also calculated, to see if a non-uniform temperature gave rise to a non-uniform lattice that would have affected the Bragg diffraction. However, calculations showed that between 150 K and 80 K the lattice spacing varied only by 5.5e-15 m, a statistically negligible change given the lattice spacing is only of the order of Angstroms. This shows that the variance of the lattice spacing directly due to temperature is unlikely to impact the Bragg diffraction.

Despite varying designs between the different crystals, the mechanical boundary conditions used stay the same; each crystal is anchored by a single fixed point in the centre of its base, with a line extending from this point to

ISBN: 978-3-95450-188-5 doi:10.18429/JACoW-MEDSI2016-TUPE10

the diffracting surface prescribed movement in the x- and y-directions. The entire crystal is also mounted to a spring foundation of ten Newtons per metre. This combination of boundary conditions enables us to model free thermal expansion, giving an accurate image of how each crystal would behave.

METHOD

Eight monochromator crystal designs were considered, varying structure and/or cooling method: the current monochromator design for Diamond's I20 beamline, a number of modifications to that crystal and then a silicon wafer. These designs are subjected to each of the incident powers in both the minimum and maximum angles of the beam footprint, i.e. at a footprint of 36 mm x 25 mm representing an incident beam angle of 30° to the crystal and at a footprint of 5 mm x 25 mm representing an incident beam angle of 6° to the crystal.

The first design modelled was the crystal currently used in Diamond Light Source's I20 beamline as shown in Fig. 1. The crystal is based on a rectangle with the top edges removed; this is to allow the beam to pass, as the I20 beamline features very little space between the monochromator crystals. The entire crystal is thermalized at 80 K, to represent liquid nitrogen cooling reaching an equilibrium.

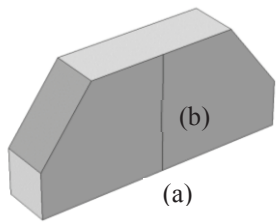

Figure 1: a cutaway view of the existing I20 monochromator crystal design. Point (a) is held fixed while line (b) is restrained in the x- and y-directions.

The next model simulated was using the same crystal design as shown in Fig. 1, but this time cooling only the bottom surface. This was to allow the heat to dissipate more evenly through the crystal, and was anticipated to produce less overall cooling and a higher peak temperature but a more uniform deformation across the diffracting region.

In order to explore alternate designs we next simulated a five-hundred-micron silicon wafer as shown in Fig. 2. Theoretically by reducing the thickness of the crystal we should allow more of the waste X-ray to pass through, reducing the thermal load on the crystal and therefore the peak temperature.

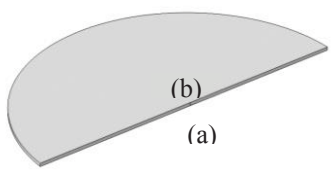

Figure 2: a cutaway view of the silicon wafer monochromator crystal design. Point (a) is held fixed while line (b) is restrained in the x- and y-directions.

RESULTS

Although eight crystal structures were modelled, in the interest of brevity we have chosen the existing crystal and the two most interesting results to explore here in depth. Figures 3, 4 and 5 show the temperature distribution and resulting deformation caused by the 1100 W power in the 30° configuration.

In the current I20 crystal with both sides cooled as well as the base, the temperature profile is drastic as shown in Fig. 3; the centre of the diffracting surface is somewhat hotter than the edges, resulting in stresses in the diffracting surface. There is high stress particularly in the centre of the diffracting region; this could cause a stress dislocation, where the lattice misaligns as a result of the stress on it. The crystal surface distorts by fifty-five picometres over a width of twenty-five millimetres, giving rise to a radius of curvature of 688,000 m (3s. f) at the centre of the diffracting surface.

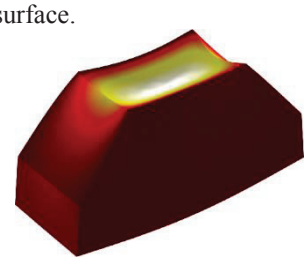

Figure 3: The current I20 monochromator after thirty second exposure to the 1100 W beam at a 30o angle of incidence.

With only the bottom cooled, we see a far more uniform temperature profile in the diffracting region as shown in Fig. 4. There is very little stress in the diffracting region; what stress is found is on the edges of the crystal and is formed by the surface contracting; in essence the crystal is attempting to curl up. Although the crystal as a whole deforms more, it is worth noting that the relative deformation of the diffracting region is largely constant due to the lack of cooling on the sides. The diffracting surface deforms by forty picometres over a width of 25 mm, giving a radius of curvature of 917,000 m (3s.f.) at the centre.

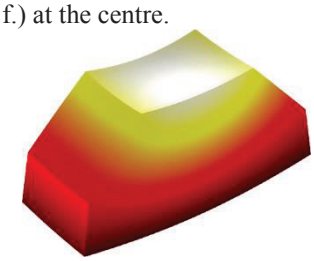

Figure 4: The current I20 monochromator cooled from the bottom only after thirty second exposure to the 1100 W beam at a 30° angle of incidence.

As theorised the thinner crystal does accomplish a slightly lower temperature than that of the current crystal design. However, due to the thinness of the crystal it bows very easily under the lower temperature as shown in Fig. 5; the diffracting surface deforms by six hundred picometres, resulting in a radius of curvature of 103,000 m (3s.f.) at the centre.

ISBN: 978-3-95450-188-5 doi:10.18429/JACoW-MEDSI2016-TUPE10

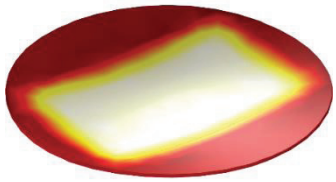

Figure 5: The silicon wafer monochromator after thirty second exposure to the 1100 W beam at a 30° angle of incidence.

CONCLUSION

To help analyse the performance of the crystals the radius of curvature of each design at each power has been plotted on Figs. 6 & 7 for the 30° and 6° angle of incidence respectively.

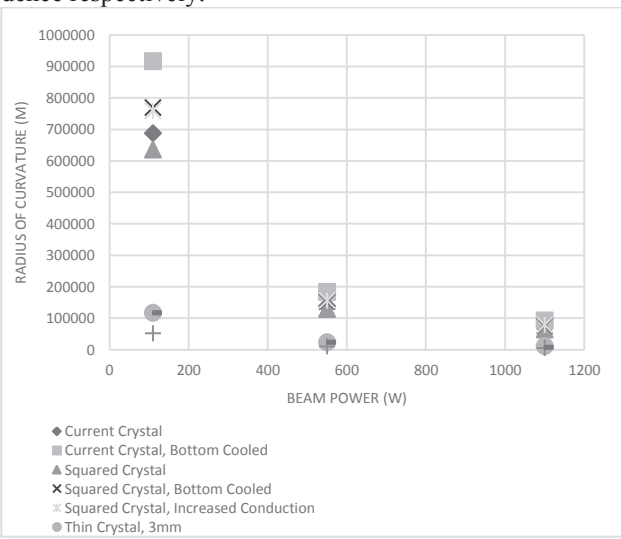

Figure 6: Radius of curvature as a function of beam power deposited in a 36 mm footprint.

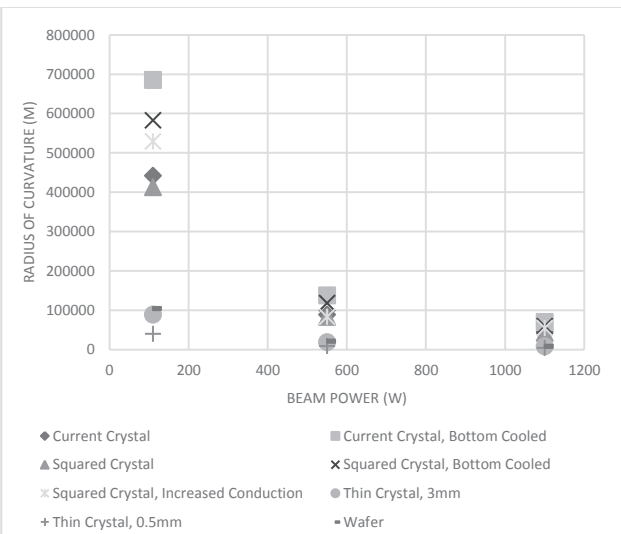

Figure 7: Radius of curvature as a function of beam power deposited in a 5mm footprint.

A common feature of all the models tested is that the thinner the crystal, the lower the maximum temperature. This is due to the heat conducting to the cooled surface in less time when the crystal is thinner. However, due to their flexibility these designs also show significant bowing with a lower radius of curvature.

The models with consistently the highest radius of curvature, and therefore the least bowing, are thicker crystals cooled from the bottom alone. This design allows the heat to dissipate more evenly, though more slowly, throughout the crystal, resulting in less variation in the deformation and a higher radius of curvature.

The next step is to explore the mechanical side of these designs; how would they be held in good thermal contact with the heat exchangers and what steps can be taken to minimise mechanical stresses upon them. Many synchrotron facilities clamp their monochromator crystals between heat exchangers to hold them in the beam path; this design is not compatible with the concept of cooling the crystal from the base alone. However, bolting directly down to a heat exchanger or cooling the bolting plate itself could cause stresses to develop in the diffracting surface as the crystal contracts from the surface. Further work is needed to ascertain the feasibility of this approach.

REFERENCES

[1] W. H. Bragg and W. L. Bragg, "The Reflexion of X-rays by Crystals," in *Proceedings of the Royal Society of London*, 1913, pp. 428–438.

[2] J. A. Golovchenko, "X-ray monochromator system for use with synchrotron radiation sources," *Rev. Sci. Instrum.*, vol. 52, no. 4, p. 509, Apr. 1981.

[3] P. Carpentier, M. Rossat, P. Charrault, J. Joly, M. Pirocchi, J. L. Ferrer, O. Kaïkati, and M. Roth, "Synchrotron monochromator heating problem, cryogenic cooling solution," *Nucl. Instruments Methods Phys. Res. Sect. A Accel. Spectrometers, Detect. Assoc. Equip.*, vol. 456, no. 3, pp. 163–176, 2001.

[4] L. Zhang, M. Sánchez Del Río, G. Monaco, C. Detlefs, T. Roth, A. I. Chumakov, and P. Glatzel, "Thermal deformation of cryogenically cooled silicon crystals under intense X-ray beams: Measurement and finite-element predictions of the surface shape," *J. Synchrotron Radiat.*, vol. 20, pp. 567–580, 2013.

[5] D. H. Bilderback, a K. Freund, G. S. Knapp, and D. M. Mills, "The historical development of cryogenically cooled monochromators for third-generation synchrotron radiation sources.," *J. Synchrotron Radiat.*, vol. 7, no. Pt 2, pp. 53–60, 2000.

[6] A. Beer, "Bestimmung der Absorption des rothen Lichts in farbigen Flüssigkeiten," *Ann. Phys.*, vol. 162, no. 5, pp. 78–88, 1852.

[7] A. Borovik and M. G. Katz, "Who Gave you the Cauchy-Weierstrass Tale? The Dual History of Rigorous Calculus." 2011.